THE JOURNAL OF PHYSICAL CHEMISTRY A

Article

pubs.acs.org/JPCA

Tetramethoxybenzene is a Good Building Block for Molecular Wires: Insights from Photoinduced Electron Transfer

Luisa G. Heinz,[†] Oleksandr Yushchenko,[‡] Markus Neuburger,[†] Eric Vauthey,*[,‡] and Oliver S. Wenger*[,†]

[†]Department of Chemistry, University of Basel, St. Johanns-Ring 19, CH-4056 Basel, Switzerland

[‡]Department of Physical Chemistry, University of Geneva, 30 quai Ernest Ansermet, CH-1211 Geneva 4, Switzerland

Supporting Information

ABSTRACT: Two donor bridge−acceptor molecules with terminal triarylamine and $Ru(bpy)_3^{2+}$ (bpy = 2,2′-bipyridine) redox partners were synthesized and investigated by cyclic voltammetry, optical absorption, luminescence, and transient absorption spectroscopy. The two dyads differ only by the central bridging unit, which was tetramethoxybenzene (tmb) in one case and unsubstituted phenylene (ph) in the other case. Photoirradiation of the $Ru(bpy)_3^{2+}$ complex of the two dyads triggers intramolecular electron transfer from the triarylamine to the ^{3}MLCT-excited metal complex, and this process occurs with time constants of 1.5 and 6.8 ns for the tmb- and ph-bridged dyads, respectively. Thermal electron transfer in the reverse direction then leads to disappearance of the photoproduct with a time constant of 10 ns in both dyads. The faster rate of photoinduced charge transfer in the tmb-bridged dyad can be understood in the framework of a hole-tunneling model in which the electron-rich tmb bridge imposes a more shallow barrier than the less electron-rich ph spacer. Until now tmb-based molecular wires have received very little attention, and alkoxy substituents have been mostly used for improving the solubility of oligo-*p*-phenylene vinylene (OPV) and oligo-*p*-phenylene ethynylene (OPE) wires. Our study illustrates how four alkoxy-substituents on a phenylene backbone can have a significant influence on the charge-transfer properties of a molecular wire, and this is relevant in the greater context of a future molecular electronics technology.

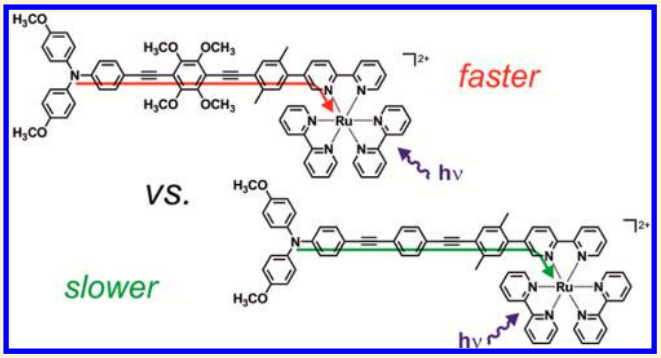

INTRODUCTION

Long-range electron transfer can occur either via tunneling or hopping mechanisms.[1−3] The latter requires redox-active units in the electron transfer pathway, which can temporarily be reduced or oxidized, and such units have sometimes been called "stepping stones".[4−6] Even though in the tunneling regime the bridge is neither oxidized nor reduced, its electronic structure plays a key role in mediating electronic coupling between the donor and the acceptor.[7−12] Many researchers have attempted to optimize molecular bridges to obtain fast electron or energy transfer over long distances (>10 Å).[10,11,13−36] In some of our own recent work we found that electron transfer from a phenothiazine donor to a photogenerated $Ru(bpy)_3^{3+}$ (bpy = 2,2′-bipyridine) species across a series of four *p*-xylene spacers proceeds with a time constant of ∼20 μs, whereas equidistant charge transfer between the same donor and acceptor across four *p*-dimethoxybenzene units occurred ∼1000 times faster (Scheme 1).[37] Dimethoxybenzene is oxidized significantly more easily than xylene, and consequently hole tunneling is associated with a more shallow barrier in the case of *p*-dimethoxybenzene than when *p*-xylene bridging units are present.[8,38,39] Related observations have been made on various systems by different researchers.[38,40−44]

Scheme 1. Hole Transfer from Photogenerated $Ru(bpy)_3^{3+}$ to Phenothiazine across *p*-Xylene and *p*-Dimethoxybenzene Spacers[37]

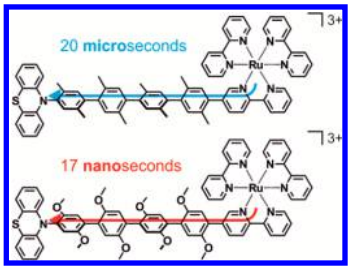

1,2,4,5-Tetramethoxybenzene (tmb) is oxidized even more readily than *p*-dimethoxybenzene,[45−47] and therefore we reasoned that a molecular bridge containing tmb might be able to mediate long-range charge transfer even more efficiently. The electrochemical potential for one-electron oxidation of tmb is in fact so low that the transition from a tunneling to a hopping regime appeared possible in

Received: April 16, 2015
Revised: April 29, 2015
Published: May 14, 2015

ACS Publications © 2015 American Chemical Society

DOI: 10.1021/acs.jpca.5b03649
J. Phys. Chem. A 2015, 119, 5676−5684

combination with a triarylamine (TAA)/$Ru(bpy)_3^{2+}$ redox couple. In a prior study we connected tmb directly to a $Ru(bpy)_3^{2+}$ complex and a neighboring *p*-dimethoxybenzene bridge unit.[48] This molecular design turned out to be suboptimal because the steric demand of tmb caused large equilibrium torsion angles between tmb and its neighboring building blocks. This is detrimental for long-range electron transfer because π-conjugation is reduced substantially when increasing the torsion angle between adjacent phenyl or pyridine rings.[12,49−51] For the present study we therefore flanked the tmb bridging unit with ethynyl groups, resulting in the **TAA-tmb-Ru^{2+}** dyad shown in Scheme 2. An analogous compound with an unsubstituted phenylene (ph) instead of the tmb unit was explored as a reference system (**TAA-ph-Ru^{2+}**).

Scheme 2. Molecular Structures of the Two Donor Bridge−Acceptor Compounds Investigated in This Work

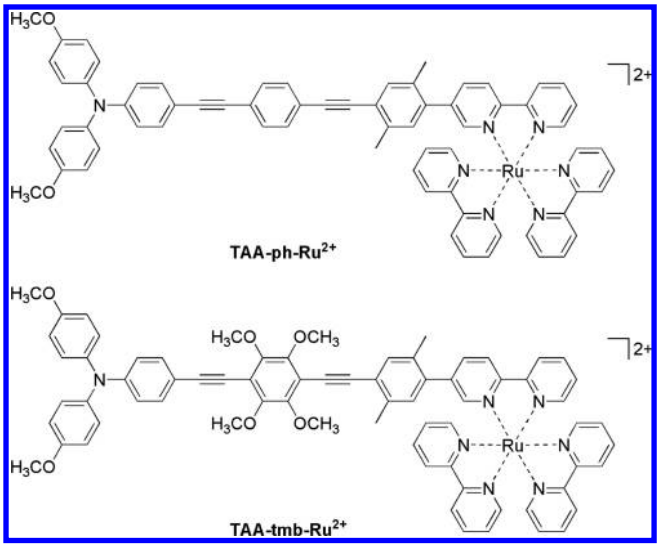

RESULTS AND DISCUSSION

Synthesis and X-ray Crystallography. The two dyads from Scheme 2 each contain a ligand in which a bpy motif is connected to a triarylamine (TAA) electron donor, either via a tmb or a ph bridging unit. These two ligands (**21** and **22**) were synthesized as illustrated by Scheme 3.

For the **TAA-tmb-Ru^{2+}** dyad, synthesis started from 2,5-dihydroxy-1,4-benzoquinone (**1**), which was converted to 1,4-diethynyl-2,3,5,6-tetramethoxybenzene (**7**) in six steps in 53% overall yield.[42,52−54] For the **TAA-ph-Ru^{2+}** dyad, the 1,4-diethynylbenzene (**10**) building block was available in only two steps from commercial 1,4-diiodobenzene (**8**) in 93% yield.[55] The iodoxylene-equipped bpy fragment **16** was accessible in three steps from commercial chemicals (**11**, **12**),[56,57] in addition to the two-step synthesis of 4-(trimethylsilyl)-phenylboronic acid (**14**) from 2,5-dibromo-*p*-xylene.[58−60] The iodo-substituted TAA unit **20** was prepared in two steps from bis(*p*-anisyl)amine (**17**) following a previously published method.[61] One-pot Sonogashira coupling reactions involving the iodo-substituted TAA donor unit **20**, diethynyl-equipped bridging units **7** or **10**, and the iodoxylene-equipped bpy fragment **16** then afforded the desired ligands **21** and **22**.

The result of an X-ray diffraction study of single crystals of ligand **21**, grown by slow evaporation from acetone solution, is shown in Figure 1. Ligand **21** crystallizes in space group $P\bar{1}$ with two molecules per unit cell. The triarylamine donor unit adopts its common propeller-shaped structure,[62] and the bipyridine ligand has its two pyridine units oriented in opposite fashion to each other, as commonly observed. The central tetramethoxybenzene unit is nearly coplanar with the adjacent phenyl rings with torsion angles of 10.1° and 34.1° relative to the *p*-xylene unit and the relevant phenyl from the triarylamine, respectively. The distance between the triarylamine N atom and the center of the bpy ligand is 22.9 Å; consequently, the N−Ru (donor−acceptor distance) in the dyad will be roughly 23 Å. Ligand **21** arranges in sheets that lie in the crystallographic *ab* plane.

UV−vis Spectroscopy and Electrochemistry. In Figure 2 the optical absorption spectra of **TAA-tmb-Ru^{2+}** and **TAA-ph-Ru^{2+}** in CH_3CN are shown along with the UV−vis spectrum of the $Ru(bpy)_3^{2+}$ reference complex measured under identical conditions. In the two dyads, the ^{1}MLCT absorption band of the photosensitizer is merely a shoulder to more intense, ligand-centered absorption bands, yet it seems likely that the lowest-energetic electronically excited state is the MLCT state of the $Ru(bpy)_3^{2+}$ fragment in both dyads.

Cyclic voltammograms obtained using solutions of the two dyads in CH_3CN in the presence of 0.1 M $TBAPF_6$ as a supporting electrolyte are shown in Figure 3. Oxidative and reductive potential sweeps with rates of 0.1 V/s were conducted separately because this gave higher quality results. In the reductive sweeps one easily recognizes three subsequent reversible waves corresponding to consecutive one-electron reduction of each of the three bpy ligands of the photosensitizer between −1.8 V and −2.2 V versus Fc^+/Fc, as commonly detected.[63−65] In the oxidative sweeps, there is a wave due to triarylamine oxidation around 0.2 V versus Fc^+/Fc and a wave caused by the Ru(II)/Ru(III) couple around 0.8 V versus Fc^+/Fc, both in line with expectation.[63−66] For the isolated 1,2,4,5-tetramethoxybenzene (tmb) molecule an oxidation potential of 0.42 V versus Fc^+/Fc has been reported,[45,46] but in Figure 3 there is no sign of tmb oxidation, perhaps because its oxidation overlaps with that of the triarylamine. All relevant reduction potentials are summarized in Table 1.

Identification of Photoproducts. In Figure 4a,d transient absorption spectra obtained after excitation of 2×10^{-5} M solutions of the two dyads in aerated CH_3CN at 532 nm with laser pulses of ∼10 ns duration are shown. The spectra were recorded by averaging over a time period of 200 ns starting immediately after the excitation pulses. Use of this wavelength leads to selective excitation of the $Ru(bpy)_3^{2+}$ photosensitizer of **TAA-tmb-Ru^{2+}** and **TAA-ph-Ru^{2+}**. For both dyads a similar transient absorption spectrum is obtained: There are absorption bands centered at 740 and 470 nm in addition to a bleach at 390 nm. These three spectral features can be explained by the formation of **TAA$^+$-tmb-Ru$^+$** and **TAA$^+$-ph-Ru$^+$** photoproducts as a result of electron transfer from TAA to the photoexcited $Ru(bpy)_3^{2+}$ complex as explained in the following.

The UV−vis difference spectra in Figure 4b,e were measured after addition of 1 equiv of $Cu(ClO_4)_2$ to solutions of **TAA-tmb-Ru^{2+}** and **TAA-ph-Ru^{2+}** in CH_3CN, which leads primarily to oxidation of the triarylamine;[66] the spectra obtained before addition of any chemical oxidant served as baselines in both cases. One observes increased absorption at ∼750 and ∼475 nm as well as decreased absorption at ∼400 nm in both dyads. The bands at ∼750 and ∼475 nm are typical for triarylamine radical cations.[57,66,69,70]

DOI: 10.1021/acs.jpca.5b03649
J. Phys. Chem. A 2015, 119, 5676−5684

Scheme 3. Synthesis of the Ligands with Triarylamine Donor Groups and tmb/ph Spacers[a]

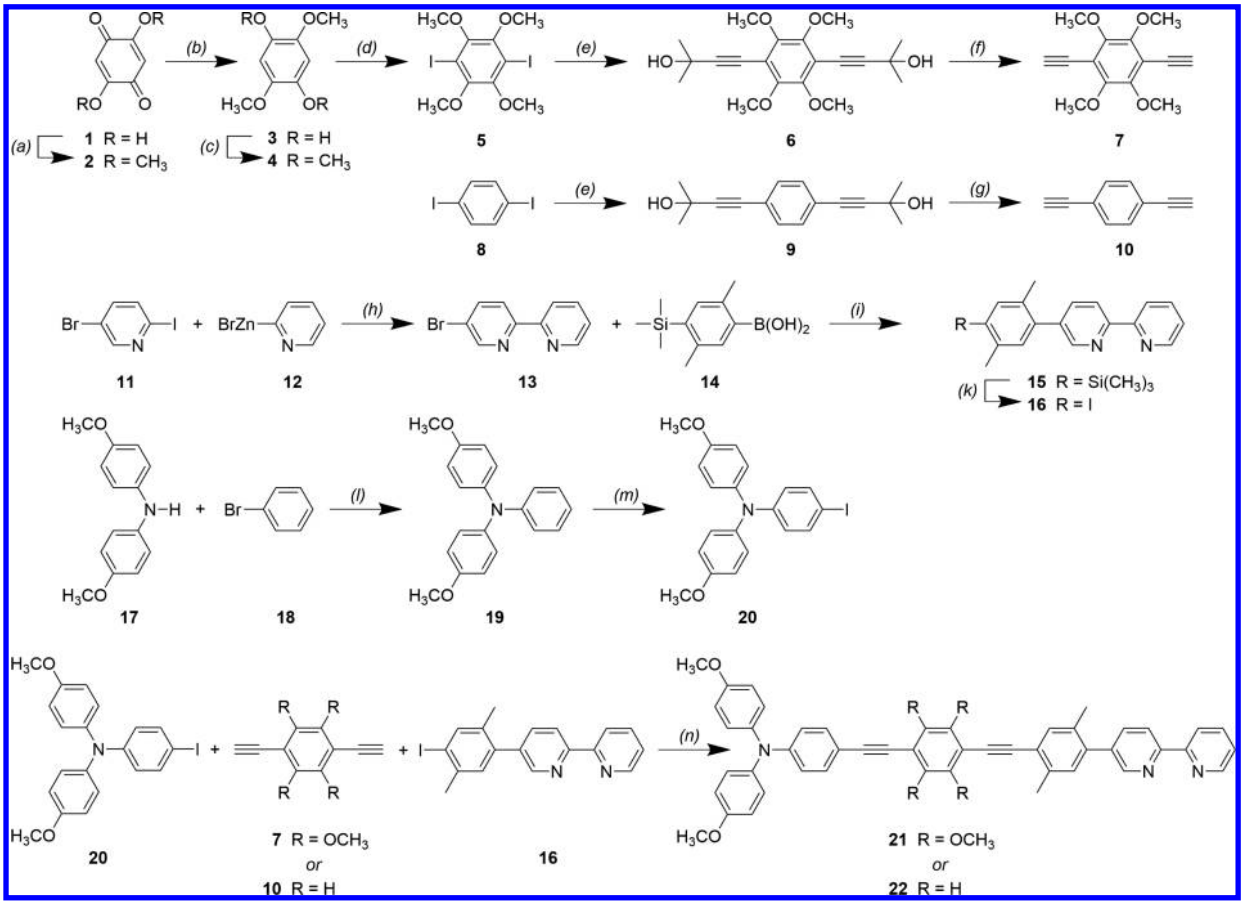

[a](a) $BF_3{\cdot}Et_2O$, MeOH; (b) $NaBH_4$, EtOH; (c) Me_2SO_4, $NaHSO_3$, KOH, EtOH/H_2O; (d) *n*-BuLi, TMEDA, Et_2O, I_2; (e) 2-methyl-3-butyn-2-ol, $PdCl_2(PPh_3)_2$, CuI, Et_3N; (f) NaH, toluene; (g) KOH, toluene; (h) $Pd(PPh_3)_4$, THF; (i) $Pd(PPh_3)_4$, Na_2CO_3, THF/H_2O; (k) ICl, CH_3CN/CH_2Cl_2; (l) NaO^tBu, $Pd(dba)_2$, $(HP^tBu_3)BF_4$, toluene; (m) $C_6H_5I(CF_3COO)_2$, I_2, CH_2Cl_2; (n) $PdCl_2(PPh_3)_2$, CuI, Et_3N.

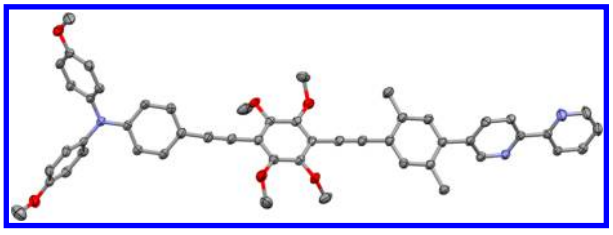

Figure 1. Crystallographic structure of ligand **21** (used for the **TAA-tmb-Ru^{2+}** dyad). Anisotropic displacement parameters are drawn at the 50% probability level.

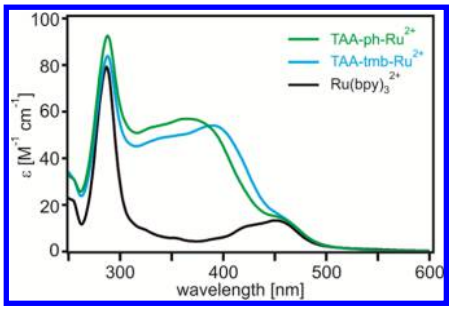

Figure 2. Optical absorption spectra of the two dyads from Scheme 2 along with the UV–vis spectrum of $Ru(bpy)_3^{2+}$ in CH_3CN.

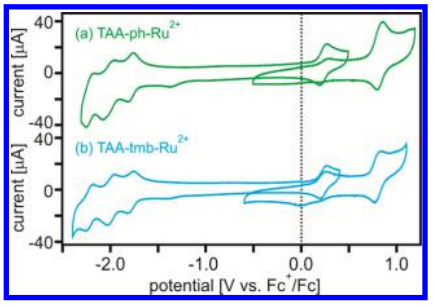

Figure 3. Cyclic voltammograms for the two dyads from Scheme 2 in CH_3CN with 0.1 M $TBAPF_6$. The potential sweep rates were 0.1 V/s.

The UV–vis difference spectra in Figure 4c,f were obtained by applying a potential of −1.8 V versus Fc^+/Fc to solutions of **TAA-tmb-Ru^{2+}** and **TAA-ph-Ru^{2+}** in CH_3CN (using a Pt grid electrode); the spectra obtained before applying any potential served as baselines in both cases. At this potential the $Ru(bpy)_3^{2+}$ unit in both dyads can be reduced selectively (Table 1). In both cases this leads to increased absorption above ∼400 nm and to a bleach at shorter wavelengths.

For both dyads the transient absorption spectra (Figure 4a,d) are essentially a 1:1 superposition of the spectro-electrochemical data illustrating the formation of TAA^+ and $Ru(bpy)_3^{+}$ ("Ru^{+}"). This is clear evidence for intramolecular electron transfer from TAA to photoexcited $Ru(bpy)_3^{2+}$ in **TAA-tmb-**

DOI: 10.1021/acs.jpca.5b03649
J. Phys. Chem. A 2015, 119, 5676–5684

Table 1. Reduction Potentials (E^0) for the Individual Redox-Active Components of the Two Dyads from Scheme 2[a]

	TAA-tmb-Ru^{2+}	TAA-ph-Ru^{2+}
Ru(III)/(II)	0.80	0.81
TAA$^{+/0}$	0.23	0.23
tmb$^{+/0}$	0.42[b,c]	
ph$^{+/0}$		2.10[d,c]
bpy$^{0/-}$	−1.78	−1.78
bpy$^{0/-}$	−1.99	−2.03
bpy$^{0/-}$	−2.21	−2.22

[a]In CH_3CN with 0.1 M $TBAPF_6$, measured with potential sweep rates of 0.1 V/s. All potentials are given in Volts relative to the Fc^+/Fc couple. [b]Reported in refs 45 and 46 for the 1,2,4,5-tetramethoxybenzene molecule in CH_3CN. [c]Converted from a potential reported in V vs SCE to V vs Fc^+/Fc according to ref 68. [d]Reported in ref 67 for the benzene molecule in CH_3CN.

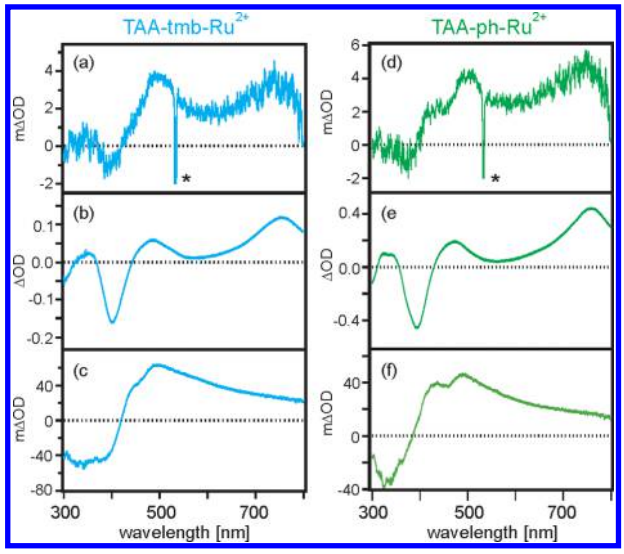

Figure 4. Transient difference spectra of (a) **TAA-tmb-Ru^{2+}** and (d) **TAA-ph-Ru^{2+}** in aerated CH_3CN (2×10^{-5} M) measured after excitation at 532 nm with laser pulses of ~10 ns duration. The signal was averaged over a time interval of 200 ns immediately after excitation. The asterisks (*) mark signals due to laser stray light. UV−vis difference spectra of (b) **TAA-tmb-Ru^{2+}** and (e) **TAA-ph-Ru^{2+}** measured in CH_3CN after addition of one equivalent of $Cu(ClO_4)_2$ as a chemical oxidant. UV−vis difference spectra of (c) **TAA-tmb-Ru^{2+}** and (f) **TAA-ph-Ru^{2+}** measured in CH_3CN after applying a potential of −1.8 V vs Fc^+/Fc to induce reduction of $Ru(bpy)_3^{2+}$ to $Ru(bpy)_3^{+}$. In (b, c, e, f) the UV−vis spectra recorded before applying any potential or before adding any chemical oxidant served as baselines.

Ru^{2+} and **TAA-ph-Ru^{2+}**. The reaction free energy (ΔG_{ET}^0) for this process can be estimated with the Weller equation (eq 1),[71] using the electrochemical potentials from Table 1 and a ^{3}MLCT energy (E_{00}) of 2.12 eV for $Ru(bpy)_3^{2+}$.[63,72] For a donor−acceptor distance (R_{DA}) of 23 Å (see above), this method yields $\Delta G_{ET}^0 = -0.13$ eV for both dyads. The reverse (thermal) electron transfer from Ru^+ back to TAA^+ to re-establish the starting materials is associated with a reaction free energy (ΔG_{bET}^0) of −1.99 eV in both dyads. Equation 2 was employed to estimate the (outer-sphere) reorganization energy (λ_o) associated with photoinduced electron transfer.[73,74] Using a reactant radius ($r_D = r_A$) of 4.5 Å and the relevant constants for CH_3CN ($\varepsilon_s = 35.94$, $n = 1.3460$) one obtains $\lambda = 1.35$ eV for both dyads.

$$\Delta G_{ET}^0 = e\cdot(E^0(TAA^{+/0}) - E^0(bpy^{0/-})) - E_{00} - e^2/(4\cdot\pi\cdot\varepsilon_0\cdot\varepsilon_s\cdot R_{DA}) \quad \text{(eq 1)}$$

$$\lambda_o = (e^2/4\cdot\pi\cdot\varepsilon_0)\cdot[(2\cdot r_D)^{-1} + (2\cdot r_A)^{-1} - R_{DA}^{-1}]\cdot(n^{-2} - \varepsilon_s^{-1}) \quad \text{(eq 2)}$$

Assuming that the total reorganization energy (λ) is dominated by the outer-sphere contribution (λ_o), this analysis then leads to the conclusion that photoinduced electron transfer from TAA to photoexcited $Ru(bpy)_3^{2+}$ takes place in the so-called normal regime in both dyads ($-\Delta G_{ET}^0 < \lambda$), whereas the reverse (thermal) electron transfer occurs in the Marcus inverted region ($-\Delta G_{bET}^0 > \lambda$). The latter process is in fact closer to the barrierless point; hence, one might anticipate more rapid thermal reverse electron transfer than photoinduced (forward) electron transfer.

Kinetics of Photoinduced Electron Transfer. A combination of pico- and nanosecond transient absorption spectroscopy was necessary to explore the electron transfer kinetics in the two dyads from Scheme 2. Following excitation at 400 nm with a femtosecond laser pulse,[75] the series of transient absorption spectra shown in Figure 5 was obtained for

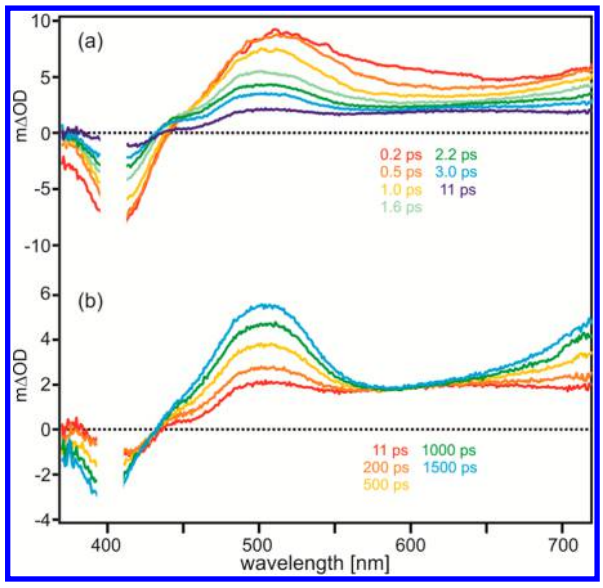

Figure 5. Transient absorption spectra measured at different time delays after excitation of **TAA-tmb-Ru^{2+}** in deaerated CH_3CN at 400 nm using a fs/ps TA setup.[75] Analogous data for the **TAA-ph-Ru^{2+}** dyad are reported in the Supporting Information (Figure S1).

TAA-tmb-Ru^{2+} in deaerated CH_3CN. An analogous data set for **TAA-ph-Ru^{2+}** is in the Supporting Information (Figure S1). On a very short time scale (<10 ps), one observes absorption maxima at 510 and 730 nm in addition to a bleach near 400 nm. The respective signals decrease over the first 11 ps (Figure 5a) before there is an increase of absorptions with maxima at 500 nm and above 700 nm, in addition to a growing bleach at 400 nm (Figure 5b). The temporal evolution of the transient absorption was analyzed by a global fit involving four exponential functions, yielding time constants of 0.9 ps, 1.4 ps, 1.6 ns, and >5 ns. Alternatively, a global target analysis assuming an A → B → C → D → E reaction scheme (with "A" the initially excited state and "E" the ground state) was performed, and this procedure yielded, as expected,[76] the same

DOI: 10.1021/acs.jpca.5b03649
J. Phys. Chem. A 2015, 119, 5676−5684

time constants in addition to the species-associated difference absorption spectra (SADS) shown in Figure 6. The SADS for

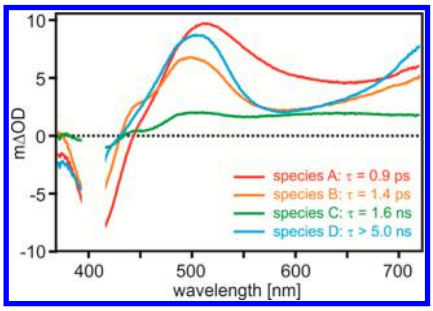

Figure 6. Species-associated difference spectra (SADS) extracted from the global target analysis of the fs/ps TA spectra measured for **TAA-tmb-Ru^{2+}** in Figure 5. Analogous SADS for **TAA-ph-Ru^{2+}** are given in the Supporting Information (Figure S2).

species D is compatible with the **TAA^{+}-B-Ru^{+}** photoproduct, and the SADS for species C is attributed to the ^{3}MLCT state of the Ru(bpy)$_3^{2+}$ unit of **TAA-B-Ru^{2+}**. Precise identification of species A and B is not possible, but the initial ultrafast processes are likely to involve internal conversion from the optically excited (ligand-centered) state to the ^{1}MLCT, intersystem crossing to the ^{3}MLCT state, and (vibrational and solvent) relaxation of the ^{3}MLCT state.[77]

For the **TAA-ph-Ru^{2+}** dyad very similar transient absorption spectra are obtained (Figure S1), but the kinetics analysis yields time constants that are different from those obtained for **TAA-tmb-Ru^{2+}**. Specifically, 0.9 ps, 1.5 ps, ∼4 ns, and >5 ns are found; the respective SADS of an A → B → C → D → E reaction sequence are shown in Figure S2. In analogy to **TAA-tmb-Ru^{2+}**, species "C" is attributed to the ^{3}MLCT state, and species "D" is assigned to the **TAA^{+}-ph-Ru^{+}** photoproduct. Given the 0−1.5 ns time window of the experimental (fs/ps) setup, only an approximate value of ∼4 ns can be estimated for the time constant for the photoinduced electron transfer process C → D.

Additional experiments, which permit detection of transient absorption spectra beyond 1.5 ns, were therefore performed on a different setup using excitation at 355 nm.[78] These experiments allow more reliable determination of the rate constants for photoinduced electron transfer (process C → D) and for thermal reverse electron transfer (process D → E). Transient absorption spectra recorded with this (sub-nanosecond/microsecond) setup at different time delays for the **TAA-tmb-Ru^{2+}** dyad in deaerated CH_3CN are shown in Figure 7. Expectedly, the same spectral features as detected above (Figure 5) are observed, but they can be followed over a significantly longer time range. On the nanosecond time scale one can identify three decay times, namely, 1.5, 10, and 560 ns. The respective SADS are shown in Figure 8. The time constant of 1.5 ns is attributed to intramolecular electron transfer from TAA to photoexcited Ru(bpy)$_3^{2+}$, and this value is in line with that extracted from the fs/ps studies (1.6 ns) reported above (Figure 5). The time constant of 10 ns is attributed to intramolecular reverse electron transfer from the reduced ruthenium photosensitizer to oxidized TAA^{+} (process D → E); to maintain consistency between Figures 5 and Figure 7, the respective species is labeled "D" in both cases. This value is more accurate than that extracted from the fs/ps studies in Figure 5; in the studies with higher temporal resolution

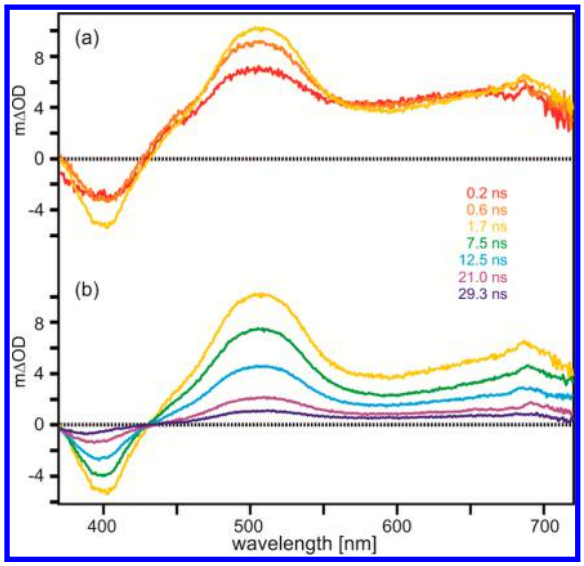

Figure 7. Transient absorption spectra measured at different time delays after excitation of **TAA-tmb-Ru^{2+}** in deaerated CH_3CN at 355 nm using a sub-nanosecond/microsecond TA setup.[78] Analogous data for the **TAA-ph-Ru^{2+}** dyad are reported in the Supporting Information (Figure S3).

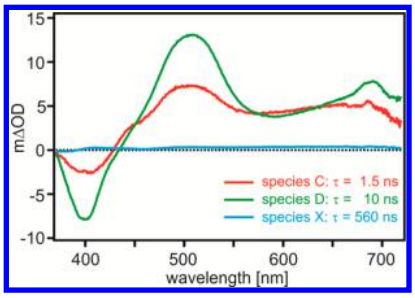

Figure 8. Species-associated difference spectra (SADS) extracted from the global target analysis of the sub-nanosecond/microsecond TA spectra measured for **TAA-tmb-Ru^{2+}** in Figure 7. Analogous SADS for **TAA-ph-Ru^{2+}** are given in the Supporting Information (Figure S4).

reported above it was merely possible to determine a lower limit of 5 ns for thermal reverse electron transfer in the **TAA-tmb-Ru^{2+}** dyad. Finally, the time constant of 560 ns is attributed to an impurity that escaped detection in the analytical methods used to characterize **TAA-tmb-Ru^{2+}** but which contributes (to a minor extent) to the transient absorption spectra in Figure 6. The respective SADS in Figure 8 is labeled with "X".

Analogous experiments were performed with the **TAA-ph-Ru^{2+}** reference dyad in CH_3CN, and the respective transient absorption spectra are reported in Figure S3. From the SADS in Figure S4, three species-associated decay times can be extracted. In this case they are 6.8, 10, and 490 ns. In analogy to the **TAA-tmb-Ru^{2+}** dyad, they are attributed to the time constants for electron transfer from TAA to ^{3}MLCT-excited Ru(bpy)$_3^{2+}$ (process C → D), to thermal reverse electron transfer (process D → E), and to a (minor) impurity, respectively. All relevant rate constants for intramolecular electron transfer are summarized in Table 2.

Physical Origin of Different Rate Constants for Photoinduced Electron Transfer. In both dyads the time constants for photoinduced electron transfer (second column in Table 2) are significantly shorter than the time constant for

DOI: 10.1021/acs.jpca.5b03649
J. Phys. Chem. A 2015, 119, 5676−5684

Table 2. Time Constants for Intramolecular Electron Transfer in Deaerated CH_3CN at 20 °C

	forward[a]	reverse[b]
TAA-tmb-Ru^{2+}	1.5 ns	10 ns
TAA-ph-Ru^{2+}	6.8 ns	10 ns

[a]Photoinduced electron transfer from TAA to ^{3}MLCT-excited $Ru(bpy)_3^{2+}$. [b]Thermal electron transfer from $Ru(bpy)_3^{+}$ to TAA^+.

thermal electron transfer in the reverse direction (third column of Table 2). At first, this finding is surprising because the driving-force and reorganization energy analysis made above suggested that thermal reverse electron transfer occurs closer to the activationless regime than photoinduced (forward) electron transfer. However, in addition to the so-called nuclear factor whose magnitude is determined by the interplay between driving-force (ΔG_{ET}^0, ΔG_{bET}^0) and reorganization energy (λ), the so-called electronic factor governs the rate constants for electron transfer.[73] As noted earlier, the electronic factor can be very different for photoinduced forward and thermal reverse electron transfer because different molecular orbitals are involved in the two processes.[7,79] We assume that it is primarily this effect that makes photoinduced electron transfer faster than thermal reverse electron transfer in our dyads.

The key finding from this study is that the equidistant intramolecular electron transfer from TAA to ^{3}MLCT-excited $Ru(bpy)_3^{2+}$ is substantially faster in **TAA-tmb-Ru^{2+}** (1.5 ns) than in **TAA-ph-Ru^{2+}** (6.8 ns). We attribute this difference to stronger electronic coupling (H_{DA}) between the TAA and $Ru(bpy)_3^{2+}$ units in the dyad with the tmb bridging unit. According to superexchange theory,[80] the electronic coupling between a donor (D) and an acceptor (A) separated by n identical bridging units (b) is given by equation 3.[1,8,38]

$$H_{DA} = \frac{h_{Db}}{\Delta\varepsilon}\cdot\left(\frac{h_{bb}}{\Delta\varepsilon}\right)^{n-1}\cdot h_{bA} \qquad \text{(eq 3)}$$

In equation 3, h_{Db}, h_{bb}, and h_{bA} represent the electronic couplings between the donor and the adjacent bridging unit, between two neighboring bridging units, and between the last bridging unit and the acceptor, respectively.[1,8] The parameter $\Delta\varepsilon$ is called tunneling energy gap and corresponds to the energy difference between the donor–acceptor system at the transition state configuration and the one-electron reduced or oxidized states of the bridge, depending on whether electron or hole transfer is considered (Scheme 4).[7,8,38,81]

In practice, $\Delta\varepsilon$ is often approximated as the difference between the donor oxidation and bridge reduction potentials when considering electron transfer, or as the difference between the acceptor reduction and bridge oxidation potentials when dealing with hole transfer.[3a,b,5a,20] In our dyads n = 1 (only single bridging units are present), and it seems plausible that the h_{Db} and h_{bA} terms in equation eq 3 are very similar for tmb and ph bridging units. However, $\Delta\varepsilon$ is expected to be substantially different for tetramethoxybenzene and unsubstituted phenylene, because the former can be oxidized significantly more easily due to its electron-donating substituents. The reduction of tmb and ph occurs at very negative potentials, and therefore it seems likely that a hole transfer rather than an electron transfer mechanism is operative in the dyads from Scheme 2. The oxidation potentials of tmb and ph are 0.42 V versus Fc^+/Fc and 2.10 V versus Fc^+/Fc, respectively (Table 1).[45,46,67] The acceptor reduction potentials are identical

Scheme 4. Illustration of the Tunneling Energy Gap ($\Delta\varepsilon$)[a]

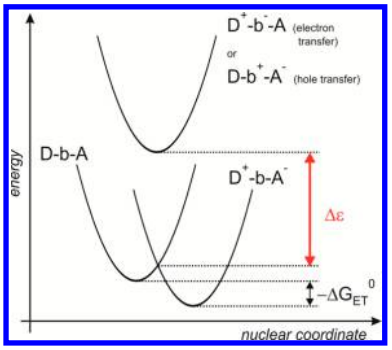

[a]D stands for donor, b stands for bridge, and A stands for acceptor. ΔG_{ET}^0 is the reaction free energy associated with electron transfer from D to A.

in **TAA-tmb-Ru^{2+}** and **TAA-ph-Ru^{2+}** and amount to −1.78 V versus Fc^+/Fc in the electronic ground state (Table 1). In the ^{3}MLCT excited state, they are 0.34 V versus Fc^+/Fc because the ^{3}MLCT energy is 2.12 eV.[63] Consequently, the estimated tunneling energy gaps are $\Delta\varepsilon$ = 0.08 eV for **TAA-tmb-Ru^{2+}** and $\Delta\varepsilon$ = 1.76 eV for **TAA-ph-Ru^{2+}**. This difference is substantial, and it can explain the difference in time constants for photoinduced electron transfer in the respective two dyads (1.5 vs 6.8 ns, Table 2).

In the superexchange model for electron transfer, the one-electron reduced or oxidized states of the bridges are never actually populated, but they are merely virtual states that define the height of the tunneling barrier associated with long-range electron transfer.[38,82] However, in the **TAA-tmb-Ru^{2+}** dyad the estimated $\Delta\varepsilon$ value is very low (0.08 eV). Given the uncertainty associated with its approximation, the possibility of a hole-hopping process in which oxidized tmb is formed as a reaction intermediate cannot be excluded a priori. However, the ultrafast time-resolved experiments reported above provide no evidence for the formation of tetramethoxybenzene cation with its characteristic absorption at 450 nm.[83] In any case it seems plausible that the low oxidation potential of tmb compared to ph plays a key role for the kinetics of photoinduced electron transfer.

Curiously, the time constants for thermal reverse electron transfer from the reduced ruthenium complex to the oxidized triarylamine are identical in both dyads (10 ns, Table 2). Assuming a hole-transfer mechanism is operative, one estimates $\Delta\varepsilon$ = 0.19 eV and $\Delta\varepsilon$ = 1.87 eV for the charge-shift from TAA^+ to tmb and ph, respectively, and this leads to the expectation of more rapid hole transfer in the tmb-bridged dyad. However, it is possible that the accelerating effect brought about by the lower $\Delta\varepsilon$ value in the tmb dyad is outbalanced by weaker electronic coupling (h_{bA}) between tmb and TAA^+ with respect to ph and TAA^+; the formation of triarylamine monocation is expected to be associated with geometrical changes that may include torsion along the C–C triple bond between tmb/ph and TAA^+, and this effect could be more pronounced in the sterically more demanding tmb unit relative to the unsubstituted ph spacer.[49,50,84]

SUMMARY AND CONCLUSIONS

Alkoxy-substituents are frequently used to improve the solubility of rigid rodlike oligo-*p*-phenylene vinylene (OPV) and oligo-*p*-phenylene ethynylene (OPE) wires.[11,13,36,85–98]

DOI: 10.1021/acs.jpca.5b03649
J. Phys. Chem. A 2015, 119, 5676–5684

Usually, the phenylene units of these oligomers or polymers are substituted with two alkoxy-groups in para-position to each other, because this leads to the desired solubility enhancement. We hypothesized that fourfold methoxy substitution would lower the oxidation potential of the resulting molecular wire to the extent that significant rate enhancement for hole transfer can be achieved. This hypothesis was verified by the comparative study of the two dyads from Scheme 2, which showed that the tetramethoxybenzene spacer of **TAA-tmb-Ru^{2+}** permits more rapid charge transfer by about a factor of 4.5 than the unsubstituted phenylene spacer of **TAA-ph-Ru^{2+}**. Consequently, fourfold alkoxy substitution might be generally beneficial in molecular wires, particularly in OPEs where the presence of more than two substituents on the phenylene units is less likely to have a detrimental effect on overall π-conjugation than in OPVs. In OPVs there might be some steric hindrance between alkoxy-groups and adjacent alkene H atoms, but at present we have no evidence that fourfold alkoxy-substitution on OPVs should not be possible.

■ ASSOCIATED CONTENT

Ⓢ Supporting Information

Synthetic protocols and product characterization data, description of equipment and methods, details from X-ray diffraction analysis of ligand **21**, additional transient absorption data. The Supporting Information is available free of charge on the ACS Publications website at DOI: 10.1021/acs.jpca.5b03649.

■ AUTHOR INFORMATION

Corresponding Authors

*E-mail: eric.vauthey@unige.ch. (E.V.)
*E-mail: oliver.wenger@unibas.ch. (O.S.W.)

Notes

The authors declare no competing financial interest.

■ ACKNOWLEDGMENTS

This work was supported by the Swiss National Science Foundation through Grant No. 200021_146231/1.

■ REFERENCES

(1) Gray, H. B.; Winkler, J. R. Long-Range Electron Transfer. *Proc. Natl. Acad. Sci. U. S. A.* **2005**, *102*, 3534−3539.

(2) Winkler, J. R.; Gray, H. B. Long-Range Electron Tunneling. *J. Am. Chem. Soc.* **2014**, *136*, 2930−2939.

(3) Weiss, E. A.; Ahrens, M. J.; Sinks, L. E.; Gusev, A. V.; Ratner, M. A.; Wasielewski, M. R. Making a Molecular Wire: Charge and Spin Transport Through *para*-Phenylene Oligomers. *J. Am. Chem. Soc.* **2004**, *126*, 5577−5584.

(4) Cordes, M.; Kottgen, A.; Jasper, C.; Jacques, O.; Boudebous, H.; Giese, B. Influence of Amino Acid Side Chains on Long-Distance Electron Transfer in Peptides: Electron Hopping via "Stepping Stones". *Angew. Chem., Int. Ed.* **2008**, *47*, 3461−3463.

(5) Malak, R. A.; Gao, Z. N.; Wishart, J. F.; Isied, S. S. Long-Range Electron Transfer across Peptide Bridges: The Transition from Electron Superexchange to Hopping. *J. Am. Chem. Soc.* **2004**, *126*, 13888−13889.

(6) Berlin, Y. A.; Hutchison, G. R.; Rempala, P.; Ratner, M. A.; Michl, J. Charge Hopping in Molecular Wires as a Sequence of Electron-Transfer Reactions. *J. Phys. Chem. A* **2003**, *107*, 3970−3980.

(7) Albinsson, B.; Eng, M. P.; Pettersson, K.; Winters, M. U. Electron and Energy Transfer in Donor-Acceptor Systems with Conjugated Molecular Bridges. *Phys. Chem. Chem. Phys.* **2007**, *9*, 5847−5864.

(8) Wenger, O. S. How Donor-Bridge-Acceptor Energetics Influence Electron Tunneling Dynamics and Their Distance Dependences. *Acc. Chem. Res.* **2011**, *44*, 25−35.

(9) Edwards, P. P.; Gray, H. B.; Lodge, M. T. J.; Williams, R. J. P. Electron Transfer and Electronic Conduction through an Intervening Medium. *Angew. Chem., Int. Ed.* **2008**, *47*, 6758−6765.

(10) Atienza-Castellanos, C.; Wielopolski, M.; Guldi, D. M.; van der Pol, C.; Bryce, M. R.; Filippone, S.; Martín, N. Determination of the Attenuation Factor in Fluorene-Based Molecular Wires. *Chem. Commun.* **2007**, 5164−5166.

(11) Fortage, J.; Goransson, E.; Blart, E.; Becker, H. C.; Hammarström, L.; Odobel, F. Strongly Coupled Zinc Phthalocyanine-Tin Porphyrin Dyad Performing Ultra-Fast Single Step Charge Separation over a 34 Angstrom Distance. *Chem. Commun.* **2007**, 4629−4631.

(12) Eng, M. P.; Albinsson, B. Non-Exponential Distance Dependence of Bridge-Mediated Electronic Coupling. *Angew. Chem., Int. Ed.* **2006**, *45*, 5626−5629.

(13) Giacalone, F.; Segura, J. L.; Martín, N.; Guldi, D. M. Exceptionally Small Attenuation Factors in Molecular Wires. *J. Am. Chem. Soc.* **2004**, *126*, 5340−5341.

(14) Harriman, A.; Ziessel, R. Making Photoactive Molecular-Scale Wires. *Chem. Commun.* **1996**, 1707−1716.

(15) Soler, M.; McCusker, J. K. Distinguishing between Dexter and Rapid Sequential Electron Transfer in Covalently Linked Donor-Acceptor Assemblies. *J. Am. Chem. Soc.* **2008**, *130*, 4708−4724.

(16) Shih, C.; Museth, A. K.; Abrahamsson, M.; Blanco-Rodriguez, A. M.; Di Bilio, A. J.; Sudhamsu, J.; Crane, B. R.; Ronayne, K. L.; Towrie, M.; Vlček, A.; et al. Tryptophan-Accelerated Electron Flow through Proteins. *Science* **2008**, *320*, 1760−1762.

(17) Meylemans, H. A.; Hewitt, J. T.; Abdelhaq, M.; Vallett, P. J.; Damrauer, N. H. Exploiting Conformational Dynamics To Facilitate Formation and Trapping of Electron-Transfer Photoproducts in Metal Complexes. *J. Am. Chem. Soc.* **2010**, *132*, 11464−11466.

(18) Schlicke, B.; Belser, P.; De Cola, L.; Sabbioni, E.; Balzani, V. Photonic Wires of Nanometric Dimensions. Electronic Energy Transfer in Rigid Rodlike $Ru(bpy)_3^{2+}$-$(ph)_n$-$Os(bpy)_3^{2+}$ Compounds (ph = 1,4-phenylene; n = 3, 5, 7). *J. Am. Chem. Soc.* **1999**, *121*, 4207−4214.

(19) Montes, V. A.; Perez-Bolivar, C.; Agarwal, N.; Shinar, J.; Anzenbacher, P. Molecular-Wire Behavior of OLED Materials: Exciton Dynamics in Multichromophoric Alq_3-Oligofluorene-Pt(II) Porphyrin Triads. *J. Am. Chem. Soc.* **2006**, *128*, 12436−12438.

(20) Montes, V. A.; Zyryanov, G. V.; Danilov, E.; Agarwal, N.; Palacios, M. A.; Anzenbacher, P. Ultrafast Energy Transfer in Oligofluorene-Aluminum Bis(8-hydroxyquinoline)acetylacetone Coordination Polymers. *J. Am. Chem. Soc.* **2009**, *131*, 1787−1795.

(21) Indelli, M. T.; Chiorboli, C.; Flamigni, L.; De Cola, L.; Scandola, F. Photoinduced Electron Transfer across Oligo-*p*-Phenylene Bridges. Distance and Conformational Effects in Ru(II)-Rh(III) Dyads. *Inorg. Chem.* **2007**, *46*, 5630−5641.

(22) Sauvage, J.-P.; Collin, J.-P.; Chambron, J.-C.; Guillerez, S.; Coudret, C.; Balzani, V.; Barigelletti, F.; De Cola, L.; Flamigni, L. Ruthenium(II) and Osmium(II) Bis(Terpyridine) Complexes in Covalently-Linked Multicomponent Systems - Synthesis, Electrochemical Behavior, Absorption Spectra, and Photochemical and Photophysical Properties. *Chem. Rev.* **1994**, *94*, 993−1019.

(23) O'Hanlon, D. C.; Cohen, B. W.; Moravec, D. B.; Dallinger, R. F.; Hopkins, M. D. Electronic, Redox, and Photophysical Consequences of Metal-for-Carbon Substitution in Oligo-Phenylene-Ethynylenes. *J. Am. Chem. Soc.* **2014**, *136*, 3127−3136.

(24) Simon, J. A.; Curry, S. L.; Schmehl, R. H.; Schatz, T. R.; Piotrowiak, P.; Jin, X. Q.; Thummel, R. P. Intramolecular Electronic Energy Transfer in Ruthenium(II) Diimine Donor Pyrene Acceptor Complexes Linked by a Single C-C Bond. *J. Am. Chem. Soc.* **1997**, *119*, 11012−11022.

(25) Baba, A. I.; Shaw, J. R.; Simon, J. A.; Thummel, R. P.; Schmehl, R. H. The Photophysical Behavior of d^6 Complexes Having Nearly

DOI: 10.1021/acs.jpca.5b03649
J. Phys. Chem. A 2015, 119, 5676−5684

Isoenergetic MLCT and Ligand Localized Excited States. *Coord. Chem. Rev.* **1998**, *171*, 43−59.
(26) Schlundt, S.; Kuzmanich, G.; Spanig, F.; Rojas, G. D.; Kovacs, C.; Garcia-Garibay, M. A.; Guldi, D. M.; Hirsch, A. Dendritic Porphyrin-Fullerene Conjugates: Efficient Light-Harvesting and Charge-Transfer Events. *Chem.—Eur. J.* **2009**, *15*, 12223−12233.
(27) Siebert, R.; Akimov, D.; Schmitt, M.; Winter, A.; Schubert, U. S.; Dietzek, B.; Popp, J. Spectroscopic Investigation of the Ultrafast Photoinduced Dynamics in pi-Conjugated Terpyridines. *ChemPhysChem* **2009**, *10*, 910−919.
(28) Vail, S. A.; Krawczuk, P. J.; Guldi, D. M.; Palkar, A.; Echegoyen, L.; Tome, J. P. C.; Fazio, M. A.; Schuster, D. I. Energy and Electron Transfer in Polyacetylene-Linked Zinc-Porphyrin-[60]Fullerene Molecular Wires. *Chem.—Eur. J.* **2005**, *11*, 3375−3388.
(29) Melomedov, J.; Ochsmann, J. R.; Meister, M.; Laquai, F.; Heinze, K. Tuning Reductive and Oxidative Photoinduced Electron Transfer in Amide-Linked Anthraquinone-Porphyrin-Ferrocene Architectures. *Eur. J. Inorg. Chem.* **2014**, *2014*, 1984−2001.
(30) Van Wallendael, S.; Rillema, D. P. Photoinduced Intramolecular Energy-Transfer from One Metal Center to the Other in a Mixed-Metal Ruthenium-Rhenium Complex. *Coord. Chem. Rev.* **1991**, *111*, 297−318.
(31) Bäuerle, P.; Segelbacher, U.; Gaudl, K. U.; Huttenlocher, D.; Mehring, M. Didodecylsexithiophene a Model-Compound for the Formation and Characterization of Charge-Carriers in Conjugated Chains. *Angew. Chem., Int. Ed.* **1993**, *32*, 76−78.
(32) He, J.; Chen, F.; Liddell, P. A.; Andreasson, J.; Straight, S. D.; Gust, D.; Moore, T. A.; Moore, A. L.; Li, J.; Sankey, O. F.; et al. Switching of a Photochromic Molecule on Gold Electrodes: Single-Molecule Measurements. *Nanotechnology* **2005**, *16*, 695−702.
(33) Liddell, P. A.; Kodis, G.; Moore, A. L.; Moore, T. A.; Gust, D. Photonic Switching of Photoinduced Electron Transfer in a Dithienylethene-Porphyrin-Fullerene Triad Molecule. *J. Am. Chem. Soc.* **2002**, *124*, 7668−7669.
(34) Zhou, G.; Baumgarten, M.; Müllen, K. Arylamine-Substituted Oligo(Ladder-Type Pentaphenylene)s: Electronic Communication Between Bridged Redox Centers. *J. Am. Chem. Soc.* **2007**, *129*, 12211−12221.
(35) Weiss, E. A.; Tauber, M. J.; Kelley, R. F.; Ahrens, M. J.; Ratner, M. A.; Wasielewski, M. R. Conformationally Gated Switching Between Superexchange and Hopping Within Oligo-*p*-Phenylene-Based Molecular Wires. *J. Am. Chem. Soc.* **2005**, *127*, 11842−11850.
(36) Tour, J. M. Conjugated Macromolecules of Precise Length and Constitution. Organic Synthesis for the Construction of Nanoarchitectures. *Chem. Rev.* **1996**, *96*, 537−553.
(37) Walther, M. E.; Wenger, O. S. Tuning the Rates of Long-Range Charge Transfer across Phenylene Wires. *ChemPhysChem* **2009**, *10*, 1203−1206.
(38) Natali, M.; Campagna, S.; Scandola, F. Photoinduced Electron Transfer Across Molecular Bridges: Electron- and Hole-Transfer Superexchange Pathways. *Chem. Soc. Rev.* **2014**, *43*, 4005−4018.
(39) Eng, M. P.; Albinsson, B. The Dependence of the Electronic Coupling on Energy Gap and Bridge Conformation − Towards Prediction of the Distance Dependence of Electron Transfer Reactions. *Chem. Phys.* **2009**, *357*, 132−139.
(40) Miller, S. E.; Lukas, A. S.; Marsh, E.; Bushard, P.; Wasielewski, M. R. Photoinduced Charge Separation Involving an Unusual Double Electron Transfer Mechanism in a Donor-Bridge-Acceptor Molecule. *J. Am. Chem. Soc.* **2000**, *122*, 7802−7810.
(41) Lambert, C.; Nöll, G.; Schelter, J. Bridge-Mediated Hopping or Superexchange Electron-Transfer Processes in Bis(Triarylamine) Systems. *Nat. Mater.* **2002**, *1*, 69−73.
(42) Hanss, D.; Walther, M. E.; Wenger, O. S. Accelerated Hole Transfer Across a Molecular Double Barrier. *Chem. Commun.* **2010**, *46*, 7034−7036.
(43) Kilså, K.; Kajanus, J.; Macpherson, A. N.; Mårtensson, J.; Albinsson, B. Bridge-Dependent Electron Transfer in Porphyrin-Based Donor-Bridge-Acceptor Systems. *J. Am. Chem. Soc.* **2001**, *123*, 3069−3080.
(44) Nelsen, S. F. Electron Transfer Reactions Within Sigma- and Pi-Bridged Dinitrogen-Centered Intervalence Radical Cations. *Adv. Phys. Organ. Chem.* **2006**, *41*, 183−215.
(45) Luo, P.; Feinberg, A. M.; Guirado, G.; Farid, S.; Dinnocenzo, J. P. Accurate Oxidation Potentials of 40 Benzene and Biphenyl Derivatives with Heteroatom Substituents. *J. Org. Chem.* **2014**, *79*, 9297−9304.
(46) Zweig, A.; Hodgson, W. G.; Jura, W. H. Oxidation of Methoxybenzenes. *J. Am. Chem. Soc.* **1964**, *86*, 4124−&.
(47) Gonzalez, M. T.; Zhao, X. T.; Manrique, D. Z.; Miguel, D.; Leary, E.; Gulcur, M.; Batsanov, A. S.; Rubio-Bollinger, G.; Lambert, C. J.; Bryce, M. R.; et al. Structural versus Electrical Functionalization of Oligo(phenylene ethynylene) Diamine Molecular Junctions. *J. Phys. Chem. C* **2014**, *118*, 21655−21662.
(48) Walther, M. E.; Wenger, O. S. Hole Tunneling and Hopping in a Ru(bpy)$_3^{2+}$-Phenothiazine Dyad with a Bridge Derived from Oligo-*p*-Phenylene. *Inorg. Chem.* **2011**, *50*, 10901−10907.
(49) Benniston, A. C.; Harriman, A. Charge on the Move: How Electron-Transfer Dynamics Depend on Molecular Conformation. *Chem. Soc. Rev.* **2006**, *35*, 169−179.
(50) Lörtscher, E.; Elbing, M.; Tschudy, M.; von Hänisch, C.; Weber, H. B.; Mayor, M.; Riel, H. Charge Transport through Molecular Rods with Reduced pi-Conjugation. *ChemPhysChem* **2008**, *9*, 2252−2258.
(51) Hanss, D.; Wenger, O. S. Conformational Effects on Long-Range Electron Transfer: Comparison of Oligo-*p*-Phenylene and Oligo-*p*-Xylene Bridges. *Eur. J. Inorg. Chem.* **2009**, 3778−3790.
(52) Viault, G.; Grée, D.; Das, S.; Yadav, J. S.; Grée, R. Synthesis of a Focused Chemical Library Based on Derivatives of Embelin, a Natural Product with Proapoptotic and Anticancer Properties. *Eur. J. Org. Chem.* **2011**, 1233−1241.
(53) Staab, H. A.; Weiser, J.; Futscher, M.; Voit, G.; Ruckemann, A.; Anders, C. Porphyrin-Quinone Cyclophanes with Gradually Varied Acceptor Strength - Syntheses and Characterizations. *Chem. Ber.* **1992**, *125*, 2285−2301.
(54) Poigny, S.; Guyot, M.; Samadi, M. Total Synthesis of Maesanin and Analogues. *Tetrahedron* **1998**, *54*, 14791−14802.
(55) Shu, W. F.; Guan, C. W.; Guo, W. H.; Wang, C. Y.; Shen, Y. J. Conjugated Poly(Aryleneethynylenesiloles) and Their Application in Detecting Explosives. *J. Mater. Chem.* **2012**, *22*, 3075−3081.
(56) Fang, Y. Q.; Hanan, G. S. Rapid and Efficient Synthesis of Functionalized Bipyridines. *Synlett* **2003**, 852−854.
(57) Hankache, J.; Wenger, O. S. Microsecond Charge Recombination in a Linear Triarylamine-Ru(bpy)$_3^{2+}$-Anthraquinone Triad. *Chem. Commun.* **2011**, *47*, 10145−10147.
(58) Hensel, V.; Lutzow, K.; Jacob, J.; Gessler, K.; Saenger, W.; Schlüter, A. D. Repetitive Construction of Macrocyclic Oligophenylenes. *Angew. Chem., Int. Ed.* **1997**, *36*, 2654−2656.
(59) Hensel, V.; Schlüter, A. D. A Biphenyl Construction Kit for Modular Chemistry. *Liebigs Ann.* **1997**, 303−309.
(60) Hanss, D.; Wenger, O. S. Tunneling Barrier Effects on Photoinduced Charge Transfer through Covalent Rigid Rod-Like Bridges. *Inorg. Chem.* **2009**, *48*, 671−680.
(61) Lambert, C.; Nöll, G.; Schmälzlin, E.; Meerholz, K.; Bräuchle, C. Synthesis, (Non)Linear Optical and Redox Properties of a Donor-Substituted Truxenone Derivative. *Chem.—Eur. J.* **1998**, *4*, 2129−2135.
(62) Bonn, A. G.; Neuburger, M.; Wenger, O. S. Photoinduced Electron Transfer in Rhenium(I)-Oligotriarylamine Molecules. *Inorg. Chem.* **2014**, *53*, 11075−11085.
(63) Vlček, A. A.; Dodsworth, E. S.; Pietro, W. J.; Lever, A. B. P. Excited-State Redox Potentials of Ruthenium Diimine Complexes - Correlations with Ground-State Redox Potentials and Ligand Parameters. *Inorg. Chem.* **1995**, *34*, 1906−1913.
(64) Juris, A.; Balzani, V.; Barigelletti, F.; Campagna, S.; Belser, P.; Von Zelewsky, A. Ru(II) Polypyridine Complexes - Photophysics, Photochemistry, Electrochemistry, and Chemi-Luminescence. *Coord. Chem. Rev.* **1988**, *84*, 85−277.
(65) Hankache, J.; Niemi, M.; Lemmetyinen, H.; Wenger, O. S. Photoinduced Electron Transfer in Linear Triarylamine-Photosensi-

DOI: 10.1021/acs.jpca.5b03649
J. Phys. Chem. A 2015, 119, 5676−5684

tizer-Anthraquinone Triads with Ruthenium(II), Osmium(II), and Iridium(III). *Inorg. Chem.* **2012**, *51*, 6333−6344.
(66) Sreenath, K.; Thomas, T. G.; Gopidas, K. R. Cu(II) Mediated Generation and Spectroscopic Study of the Tris(4-anisyl)amine Radical Cation and Dication. Unusually Shielded Chemical Shifts in the Dication. *Org. Lett.* **2011**, *13*, 1134−1137.
(67) Merkel, P. B.; Luo, P.; Dinnocenzo, J. P.; Farid, S. Accurate Oxidation Potentials of Benzene and Biphenyl Derivatives via Electron-Transfer Equilibria and Transient Kinetics. *J. Org. Chem.* **2009**, *74*, 5163−5173.
(68) Pavlishchuk, V. V.; Addison, A. W. Conversion Constants for Redox Potentials Measured Versus Different Reference Electrodes in Acetonitrile Solutions at 25 Degrees C. *Inorg. Chim. Acta* **2000**, *298*, 97−102.
(69) Geiss, B.; Lambert, C. A Small Cationic Donor-Acceptor Iridium Complex with a Long-Lived Charge-Separated State. *Chem. Commun.* **2009**, 1670−1672.
(70) Lambert, C.; Nöll, G. The Class II/III Transition in Triarylamine Redox Systems. *J. Am. Chem. Soc.* **1999**, *121*, 8434−8442.
(71) Weller, A. Photoinduced Electron-Transfer in Solution - Exciplex and Radical Ion-Pair Formation Free Enthalpies and Their Solvent Dependence. *Z. Phys. Chem.* **1982**, *133*, 93−98.
(72) Roundhill, D. M. *Photochemistry and Photophysics of Metal Complexes;* Plenum Press: New York, 1994.
(73) Marcus, R. A.; Sutin, N. Electron Transfers in Chemistry and Biology. *Biochim. Biophys. Acta* **1985**, *811*, 265−322.
(74) Barbara, P. F.; Meyer, T. J.; Ratner, M. A. Contemporary Issues in Electron Transfer Research. *J. Phys. Chem.* **1996**, *100*, 13148−13168.
(75) Banerji, N.; Duvanel, G.; Perez-Velasco, A.; Maity, S.; Sakai, N.; Matile, S.; Vauthey, E. Excited-State Dynamics of Hybrid Multichromophoric Systems: Toward an Excitation Wavelength Control of the Charge Separation Pathways. *J. Phys. Chem. A* **2009**, *113*, 8202−8212.
(76) van Stokkum, I. H. M.; Larsen, D. S.; van Grondelle, R. Global and Target Analysis of Time-Resolved Spectra. *Biochim. Biophys. Acta* **2004**, *1657*, 82−104.
(77) Sun, Q. C.; Mosquera-Vazquez, S.; Daku, L. M. L.; Guénée, L.; Goodwin, H. A.; Vauthey, E.; Hauser, A. Experimental Evidence of Ultrafast Quenching of the ^{3}MLCT Luminescence in Ruthenium(II) Tris-bipyridyl Complexes via a ^{3}dd State. *J. Am. Chem. Soc.* **2013**, *135*, 13660−13663.
(78) Lang, B.; Mosquera-Vazquez, S.; Lovy, D.; Sherin, P.; Markovic, V.; Vauthey, E. Broadband Ultraviolet-Visible Transient Absorption Spectroscopy in the Nanosecond to Microsecond Time Domain with Sub-Nanosecond Time Resolution. *Rev. Sci. Instrum.* **2013**, *84*.
(79) Yonemoto, E. H.; Riley, R. L.; Kim, Y. I.; Atherton, S. J.; Schmehl, R. H.; Mallouk, T. E. Photoinduced Electron-Transfer in Covalently Linked Ruthenium Tris(Bipyridyl) Viologen Molecules - Observation of Back Electron-Transfer in the Marcus Inverted Region. *J. Am. Chem. Soc.* **1992**, *114*, 8081−8087.
(80) McConnell, H. M. Intramolecular Charge Transfer In Aromatic Free Radicals. *J. Chem. Phys.* **1961**, *35*, 508−515.
(81) Tong, G. S. M.; Kurnikov, I. V.; Beratan, D. N. Tunneling Energy Effects on GC Oxidation in DNA. *J. Phys. Chem. B* **2002**, *106*, 2381−2392.
(82) Pettersson, K.; Wiberg, J.; Ljungdahl, T.; Mårtensson, J.; Albinsson, B. Interplay Between Barrier Width and Height in Electron Tunneling: Photoinduced Electron Transfer in Porphyrin-Based Donor-Bridge-Acceptor Systems. *J. Phys. Chem. A* **2006**, *110*, 319−326.
(83) Sato, H.; Guengerich, F. P. Oxidation of 1,2,4,5-Tetramethoxybenzene to a Cation Radical by Cytochrome P450. *J. Am. Chem. Soc.* **2000**, *122*, 8099−8100.
(84) Benniston, A. C.; Harriman, A.; Li, P.; Patel, P. V.; Sams, C. A. Electron Exchange in Conformationally Restricted Donor-Spacer-Acceptor Dyads: Angle Dependence and Involvement of Upper-Lying Excited States. *Chem.—Eur. J.* **2008**, *14*, 1710−1717.
(85) Lloveras, V.; Vidal-Gancedo, J.; Figueira-Duarte, T. M.; Nierengarten, J. F.; Novoa, J. J.; Mota, F.; Ventosa, N.; Rovira, C.; Veciana, J. Tunneling versus Hopping in Mixed-Valence Oligo-*p*-Phenylenevinylene Polychlorinated Bis(triphenylmethyl) Radical Anions. *J. Am. Chem. Soc.* **2011**, *133*, 5818−5833.
(86) Ziener, U.; Godt, A. Synthesis and Characterization of Monodisperse Oligo(phenyleneethynylene)s. *J. Org. Chem.* **1997**, *62*, 6137−6143.
(87) Davis, W. B.; Svec, W. A.; Ratner, M. A.; Wasielewski, M. R. Molecular-Wire Behaviour in p-Phenylenevinylene Oligomers. *Nature* **1998**, *396*, 60−63.
(88) Smalley, J. F.; Sachs, S. B.; Chidsey, C. E. D.; Dudek, S. P.; Sikes, H. D.; Creager, S. E.; Yu, C. J.; Feldberg, S. W.; Newton, M. D. Interfacial Electron-Transfer Kinetics of Ferrocene through Oligophenyleneethynylene Bridges Attached to Gold Electrodes as Constituents of Self-Assembled Monolayers: Observation of a Nonmonotonic Distance Dependence. *J. Am. Chem. Soc.* **2004**, *126*, 14620−14630.
(89) Pettersson, K.; Kyrychenko, A.; Ronnow, E.; Ljungdahl, T.; Martensson, J.; Albinsson, B. Singlet Energy Transfer in Porphyrin-Based Donor-Bridge-Acceptor Systems: Interaction between Bridge Length and Bridge Energy. *J. Phys. Chem. A* **2006**, *110*, 310−318.
(90) Eng, M. P.; Ljungdahl, T.; Martensson, J.; Albinsson, B. Triplet Excitation Energy Transfer in Porphyrin-Based Donor-Bridge-Acceptor Systems with Conjugated Bridges of Varying Length: An Experimental and DFT Study. *J. Phys. Chem. B* **2006**, *110*, 6483−6491.
(91) Myahkostupov, M.; Piotrowiak, P.; Wang, D.; Galoppini, E. Ru(II)-Bpy Complexes Bound to Nanocrystalline TiO_2 Films through Phenyleneethynylene (OPE) Linkers: Effect of the Linkers Length on Electron Injection Rates. *J. Phys. Chem. C* **2007**, *111*, 2827−2829.
(92) Clifford, J. N.; Gu, T.; Nierengarten, J. F.; Armaroli, N. Photoinduced Energy and Electron Transfer in Fullerene-Oligophenyleneethynylene Systems: Dependence on the Substituents of the Oligomer Unit. *Photochem. Photobiol. Sci.* **2006**, *5*, 1165−1172.
(93) de la Torre, G.; Giacalone, F.; Segura, J. L.; Martín, N.; Guldi, D. M. Electronic Communication Through pi-Conjugated Wires in Covalently Linked Porphyrin/C-60 Ensembles. *Chem.—Eur. J.* **2005**, *11*, 1267−1280.
(94) Davis, W. B.; Ratner, M. A.; Wasielewski, M. R. Conformational Gating of Long Distance Electron Transfer Through Wire-Like Bridges in Donor-Bridge-Acceptor Molecules. *J. Am. Chem. Soc.* **2001**, *123*, 7877−7886.
(95) Beckers, E. H. A.; van Hal, P. A.; Schenning, A.; El-ghayoury, A.; Peeters, E.; Rispens, M. T.; Hummelen, J. C.; Meijer, E. W.; Janssen, R. A. J. Singlet-Energy Transfer in Quadruple Hydrogen-Bonded Oligo(p-Phenylenevinylene)-Fullerene Dyads. *J. Mater. Chem.* **2002**, *12*, 2054−2060.
(96) Huber, R.; González, M. T.; Wu, S.; Langer, M.; Grunder, S.; Horhoiu, V.; Mayor, M.; Bryce, M. R.; Wang, C. S.; Jitchati, R.; et al. Electrical Conductance of Conjugated Oligomers at the Single Molecule Level. *J. Am. Chem. Soc.* **2008**, *130*, 1080−1084.
(97) Duvanel, G.; Grilj, J.; Vauthey, E. Ultrafast Long-Distance Excitation Energy Transport in Donor-Bridge-Acceptor Systems. *J. Phys. Chem. A* **2013**, *117*, 918−928.
(98) Linton, K. E.; Fox, M. A.; Palsson, L. O.; Bryce, M. R. Oligo(*p*-phenyleneethynylene) (OPE) Molecular Wires: Synthesis and Length Dependence of Photoinduced Charge Transfer in OPEs with Triarylamine and Diaryloxadiazole End Groups. *Chem.—Eur. J.* **2015**, *21*, 3997−4007.

DOI: 10.1021/acs.jpca.5b03649
J. Phys. Chem. A 2015, 119, 5676−5684